THE JOURNAL OF BIOLOGICAL CHEMISTRY
Vol. 280, No. 18, Issue of May 6, pp. 18368–18374, 2005
Printed in U.S.A.
© 2005 by The American Society for Biochemistry and Molecular Biology, Inc.

# Stepping Transfer Messenger RNA through the Ribosome*

Received for publication, August 9, 2004, and in revised form, February 9, 2005
Published, JBC Papers in Press, February 15, 2005, DOI 10.1074/jbc.M409094200

**Olga V. Shpanchenko‡§, Maria I. Zvereva‡, Pavel V. Ivanov‡¶‖, Elizaveta Y. Bugaeva‡, Alexey S. Rozov‡, Alexey A. Bogdanov‡, Markus Kalkum**, Leif A. Isaksson‡‡§§, Knud H. Nierhaus¶, and Olga A. Dontsova‡¶¶**

*From the ‡Department of Chemistry, M. V. Lomonosov Moscow State University, 119899, Moscow, Russia, ¶Max-Planck-Institut für Molekulare Genetik, AG Ribosomen, Ihnestrasse 73, D-14195 Berlin, Germany, **Immunology Division, The Beckman Research Institute of the City of Hope, Duarte, California 91010-3000, and ‡‡Department of Genetics, Microbiology, and Toxicology, Stockholm University, S-10691 Stockholm, Sweden*

**tmRNA (transfer messenger RNA) is a unique molecule used by all bacteria to rescue stalled ribosomes and to mark unfinished peptides with a specific degradation signal. tmRNA is recruited by arrested ribosomes in which it facilitates the translational switch from cellular mRNA to the mRNA part of tmRNA. Small protein B (SmpB) is a key partner for the *trans*-translation activity of tmRNA both *in vivo* and *in vitro*. It was shown that SmpB acts at the initiation step of the *trans*-translation process by facilitating tmRNA aminoacylation and binding to the ribosome. Little is known about the subsequent steps of *trans*-translation. Here we demonstrated the first example of an investigation of tmRNA·ribosome complexes at different stages of *trans*-translation. Our results show that the structural element at the position of tmRNA pseudoknot 3 remains intact during the translation of the mRNA module of tmRNA and that it is localized on the surface of the ribosome. At least one SmpB molecule remains bound to a ribosome·tmRNA complex isolated from the cell when translation is blocked at different positions within the mRNA part of tmRNA.**

tmRNA[1] (SsrA RNA or 10 S RNA (1)) is a small stable RNA that is found in all eubacteria as well as in some chloroplasts and mitochondria (2, 3). Its 3′- and 5′-ends are folded into a tRNA-like structure with an amino acid acceptor stem that possesses identity elements of $tRNA^{Ala}$ and enables specific aminoacylation of the tmRNA by alanyl-tRNA synthetase (4, 5). tmRNA has a short open reading frame in the middle of the molecule surrounded by pseudoknots (the mRNA module) that encodes a degradation signal (tag peptide) (6) for certain cellular proteases (ClpXP, ClpAP) (7). The combination of properties for both tRNA and mRNA results in an unusual translational mechanism for this molecule known as "*trans*-translation," switching translation from cellular mRNA lacking stop codon to the coding part of tmRNA, thus adding the tag peptide to the truncated polypeptide chain (8).

Several proteins were shown to function during the initiation of tmRNA-mediated *trans*-translation. Elongation factor Tu is important for initial tmRNA binding to the ribosome (9) and may also facilitate the structural rearrangement of the tmRNA molecule (10). Ribosomal protein S1 may bind to the mRNA part of tmRNA (11) in a manner similar to that of cellular mRNA (12). Small protein B (SmpB) is the only key protein known to be essential and specific for *trans*-translation. Both *in vivo* and *in vitro* studies have shown that *trans*-translation does not take place in the absence of SmpB (13, 14). This protein also facilitates tmRNA aminoacylation (15). Recently, it was shown that all SmpB molecules are bound to ribosomes within the cell. Moreover, one ribosome can bind two protein molecules that remain bound to the ribosome even after the transfer of undersynthesized peptide to tmRNA (16). SmpB was also found to be the partner of tmRNA on entering the ribosome during the pre-accommodation stage (17). Comparison of the x-ray crystal structure of a ribonucleoprotein complex that includes **a** tmRNA fragment and SmpB (18) with cryo-electron microscopic (cryo-EM) data for tmRNA·SmpB complex entering the ribosome (17) shows that SmpB protein may change its position within the tmRNA.

The interaction of tmRNA with the ribosome was studied by cryo-EM only at the pre-accommodation stage (17). Little is known about such interactions at later stages of *trans*-translation. Recently we proposed a hypothetical model describing how tmRNA may first enter and than pass through the ribosome (19). The predicted conformation of tmRNA at the initial stage of its interaction with the ribosome was confirmed by cryo-EM (17). According to our model, several structural elements of tmRNA should remain intact during the passage of tmRNA through the ribosome, and they should be located on the surface of ribosome (19). Here, we have presented the first example of *trans*-translation study at different stages of the passage of tmRNA through ribosome based on the isolation and investigation of tmRNA·ribosome complexes in which ribosomes stopped at the 4th or 11th codon of the coding part of tmRNA.

## EXPERIMENTAL PROCEDURES

*Strains*—The XL-1 strain of *Escherichia coli* was used for all of the genetic manipulations. X91 strain (ΔssrA) (20) was a kind gift of Dr. K. Williams. The SKZ-1 strain of *E. coli* with disrupted tmRNA gene and thermosensitive RF2 was made and used for the isolation of tmRNA·ribosome complex as follows. The chromosomal *prfB*+ gene of *E.*

* This work was supported in part by Grant 55000303 from the Howard Hughes Medical Institute, by Grant 02-04-48781 from the Russian Foundation for Basic Research, and Grant 1707.2003.4 from the President of the Russian Federation. The costs of publication of this article were defrayed in part by the payment of page charges. This article must therefore be hereby marked "*advertisement*" in accordance with 18 U.S.C. Section 1734 solely to indicate this fact.

§ Supported by European Molecular Biology Organization short term fellowship ASTF 69-02.

‖ Supported by a stipendium from the Max Planck Institute for Molecular Genetics (Berlin).

§§ Supported by grants from the Swedish Institute and the Swedish Research Council.

¶¶ Author to whom correspondence should be addressed. Tel.: 7-095-932-88-24; Fax: 7-095-939-31-81; E-mail: dontsova@genebee.msu.su.

[1] The abbreviations used are: tmRNA, transfer messenger RNA; SmpB, small protein B; MS, mass spectrometry; MS/MS, tandem MS; MALDI, matrix-assisted laser desorption ionization; cryo-EM, cryo-electron microscopic; IPTG, isopropyl 1-thio-β-D-galactopyranoside; DIG, digoxigenin; pk, pseudoknot; RF, release factor; Tricine, *N*-[2-hydroxy-1,1-bis(hydroxymethyl)ethyl]glycine.


This paper is available on line at http://www.jbc.org

This is an Open Access article under the CC BY license.

*coli* X91 (20) was replaced with the *prfB2* allele by co-transduction with the nearby *zgc21*::*Tn10* marker that gave tetracycline resistance, using phage P1 and UY2687 as a donor strain (21). The transduction was performed according to a standard procedure (22). To do that, a P1 stock was made in UY2687 cells. Strain X91 was than used as a recipient, and selection was made for tetracycline resistance. Co-transduction of the *prfB2* allele was determined by screening for decreased ability to grow on low salt LB at 42 °C. The absence of *ssrA* gene in the resulting strain SKZ-1 was confirmed by PCR as described previously (20).

*Plasmids*—To remove the sequence corresponding to pseudoknot 3 (pk3) and to introduce the KpnI and SmaI sites for the subsequent cloning of streptavidin-binding aptamer, two fragments of tmDNA were amplified by PCR from the plasmid pGEM-ssrA (19) in the presence of DNA primers 5′-GAG ATC GCG TGG AAG CCC GGT ACC CCC GGG TAC TCA GGC TAG TTT GTT AGT GGC-3′ and 5′-GGC AAG CTT ACT TCG CGG GAC AAA TTG-3′ (Pri2), and 5′-GCC ACT AAC AAA CTA GCC TGA GTA CCC GGG GGT ACC GGG CTT CCA CGC GAT CTC-5′ and 5′-GCG GGA TCC TAA CGA TAA CGC CAT TGA G-3′ (Pri1), respectively. After annealing, the recessed DNA 3′-ends were filled by Klenow fragment, and tmDNA was amplified by PCR in the presence of Pri1 and Pri2 oligonucleotides. This DNA was digested with BamHI and HindIII and cloned into BamHI-HindIII-digested pGEM-ssrA resulting in the pGEM-500 plasmid. pGEM-500, cut with KpnI and SmaI, was ligated with annealed oligonucleotides coding for streptavidin-binding aptamer (23) carrying the KpnI and SmaI sites in the ends. The resulting plasmid was named pGEM-stra. pGEM-stra-11 and pGEM-stra-4 coding for tmRNA-11 and tmRNA-4, respectively, with mutated termination signals (stop codons in position 4 and 11 of the tag sequence) as well as pGEM-tmRNA-$His_6$ coding for tag peptide containing 6 His residues were constructed using the QuikChange site-directed mutagenesis kit (Stratagene). Mutant sequences were verified by DNA sequencing.

*In Vivo Functional Assays*—The activities of the mutant tmRNA-4 and tmRNA-11 were tested as described in the Williams system (20) with some modifications. The plasmid pACYC184 was digested by NcoI and PvuII to delete the chloramphenicol-acetyltransferase gene. The functional domain represented by fragment coding the kanamycin resistance gene and the phage P22 Arc repressor gene lacking the stop codon and controlled by a tac promoter was subcloned from plasmid p6A (kindly provided by Dr. K. Williams) into plasmid pACYC184 with deleted chloramphenicol-acetyltransferase gene using standard techniques. The resulting plasmid p6B was transformed together with the plasmid encoding tmRNA into *E. coli* strain X91 (ΔssrA). The activity of mutant tmRNA molecules *in vivo* was tested using standard selective plates containing LB agar with 50 μg/ml ampicillin, 100 μg/ml kanamycin, 25 μg/ml tetracycline, and 1 mM IPTG and compared with wild-type tmRNA (plasmid pGEM-ssrA) (Fig. 2*A*).

To test the *trans*-translation activity, the SKZ1 strain was transformed with pGEM-tmRNA-6His. In control experiments the X91 strain was transformed with the same plasmid. The cells with or without the plasmid were grown at 37 °C to 0.6 $A_{600}$ units/ml, and protein content was analyzed by standard gel electrophoresis followed by Western blot using anti-($His_6$) antibodies.

*Complex Preparation and Affinity Purification*—For complex isolation, SKZ-1 cells carrying the appropriate plasmids were grown in low salt LB medium (1 g of NaCl/liter) at 37 °C to 0.3 $A_{600}$ units/ml. The temperature was increased to 42 °C, and after 2 h the cells were quickly cooled and harvested by centrifugation. Cell lysates were obtained as described (24), and the ribosomal fraction was purified via centrifugation through a sucrose cushion using 10/30% sucrose in buffer A, containing 20 mM Hepes-KOH, pH 7.6, 10 mM magnesium acetate, 100 mM $NH_4Cl$, and 4 mM 2-mercaptoethanol, for 18 h at 4 °C and 35,000 rpm in Ti70 rotor (Beckman). The ribosomal pellet was rinsed with buffer A and resuspended under continuous gentle stirring for about 2 h. We call these ribosomes the "initial ribosomal fraction." Approximately 10 nmol of this initial ribosomal fraction was incubated with 500 μl of streptavidin-Sepharose (Amersham Biosciences) for about 12 h at 4 °C in a 2-ml tube. The resin was washed several times with buffer A until the release of the ribosomes into the wash solution became negligible; this was determined by monitoring its absorption at 260 nm. The elution was carried out for 4 h using 0.5 ml of biotin-saturated buffer A (~220 μg/ml). The stability of the isolated complex was tested by sucrose gradient centrifugation. The complex sedimented as a single 70 S peak. No tmRNA appeared in the top fraction of the gradient as confirmed by gel electrophoretic analysis (data not shown).

*RNA Content of the Complex*—The RNA fraction of the complex was analyzed by electrophoresis following phenol extraction (25) using a 5% polyacrylamide 7 M urea denaturing gel (19:1 (w/w) monomer to bisacrylamide). The RNAs were stained with methylene blue. The semi-dry method was applied to transfer RNA onto a Hybond-N+ membrane (Amersham Biosciences) for subsequent Northern hybridization. RNA was visualized using digoxigenin (DIG) reagents for nonradioactive nucleic acid labeling and detection system (Roche Applied Science) according to the manufacturer's instructions. The DIG-labeled DNA probes used were a 404-bp-long fragment complementary to tmRNA, carrying an aptamer with high affinity for streptavidin, and a 75-bp-long fragment complementary to $tRNA^{Pro}$. The probes were prepared by PCR using DIG-dUTP (Roche Applied Science) and pGEM-stra or *E. coli* genomic DNA as a template for the synthesis of the 404-bp-long fragment and the 75-bp-long fragment, respectively.

*Protein Content of the Complex*—After trichloroacetic acid precipitation proteins were separated in 17.5% Tricine-SDS-PAGE (26) and stained with Coomassie Blue R-250.

For quantitative analysis of SmpB content the purified SmpB-$His_6$ protein (kindly provided by Y. Teraoka) was used. Certain amounts of SmpB and TP70 as well as the proteins from the complex were separated in the same gel. The intensities of the bands corresponding to SmpB and ribosomal protein L2 were determined by scanning with the Gel Explorer 1.0 program. The ratio of intensities of L2 to SmpB was estimated as 2.9 ± 0.3. This coefficient was used to normalize the experimental ratio of L2 to SmpB intensities in the case of each complex to determine the molar ratio of L2/SmpB.

*Mass Spectrometric (MS) Analyses*—A protein band at approximately 18–19 kDa (Fig. 4, *A* and *B*) cut from the protein gel was subjected to reduction, alkylation, trypsin digestion, and peptide purification as described previously (27). Desalted peptides were transferred onto a MALDI-MS sample plate, mixed with the MALDI matrix 4-hydroxy-α-cyanocinnamic acid, and allowed to dry. Mass measurements were performed on an orthogonal MALDI-quadrupole time-of-flight mass spectrometer, a prOTOF2000 (PerkinElmer Life Sciences/Sciex), within the *m/z* range from 500 to 10,000. External calibration on the monoisotopic masses of bradykinin fragment 2–9 (*m/z* 904.4681, Bachem) and pyro-E-neurotensin (*m/z* 1672.9175, Bachem) resulted in an average mass accuracy below 6.0 ppm for signals of the peptide ions observed. Peptide mass fingerprints were analyzed using Xproteo (www.xproteo.com).

Multistage MS analysis (MS/MS and $MS^3$) were performed subsequently on the same samples using a self-built MALDI-ion trap that consists of an LCQ DECA ion trap (ThermoElectron) with a customized ion source, essentially as described previously for an LCQ version (27). The machine was further improved by adding the capability to accommodate the sample plates from the prOTOF2000 and to operate at a higher source pressure (170 millitorr), which allowed us to perform measurements with 4-hydroxy-α-cyanocinnamic acid matrix. The fragmentation spectrum of the tryptic SmpB peptide ion at *m/z* 1250.67 (Fig. 5) was utilized as a characteristic signature to detect SmpB in hypothesis-driven multistage MS experiments in a fashion similar to that described for the detection of low-abundant peptides (28). These experiments were necessary to test for the presence of SmpB in cases in which peptide mass fingerprints alone did not permit a conclusive identification.

## RESULTS

*tmRNA Mutants*—An aptamer affinity tag was inserted into the tmRNA molecule to allow the isolation of tmRNA·ribosome complexes by affinity chromatography. Earlier we demonstrated that the aptamer to streptavidin was very efficient for the isolation of ribosomes when inserted into 23S rRNA (29). It is known that pk3 is absent in the tmRNAs from some eubacteria (2) and that substitution of this pseudoknot in *E. coli* tmRNA with a single-stranded structure element does not significantly affect the activity of tmRNA (30). We substituted pk3 with the aptamer to streptavidin (Fig. 1). According to our model describing the passage of tmRNA through the ribosome (19) pk3 should be located on the surface of the ribosome. Insertion of the aptamer into the pk3 position made the resultant mutant tmRNA 41 nucleotides longer than the wild type. We used the resulting plasmid pGEM-stra to express mutant tmRNA-stra (a tmRNA containing a streptavidin tag and a wild-type mRNA module) under control of its native promoter and terminator. Mutant tmRNA remained active in the test system (20).

The aptamer-tagged tmRNA mutants were designed in a way to block the translation of the coding region of tmRNA at

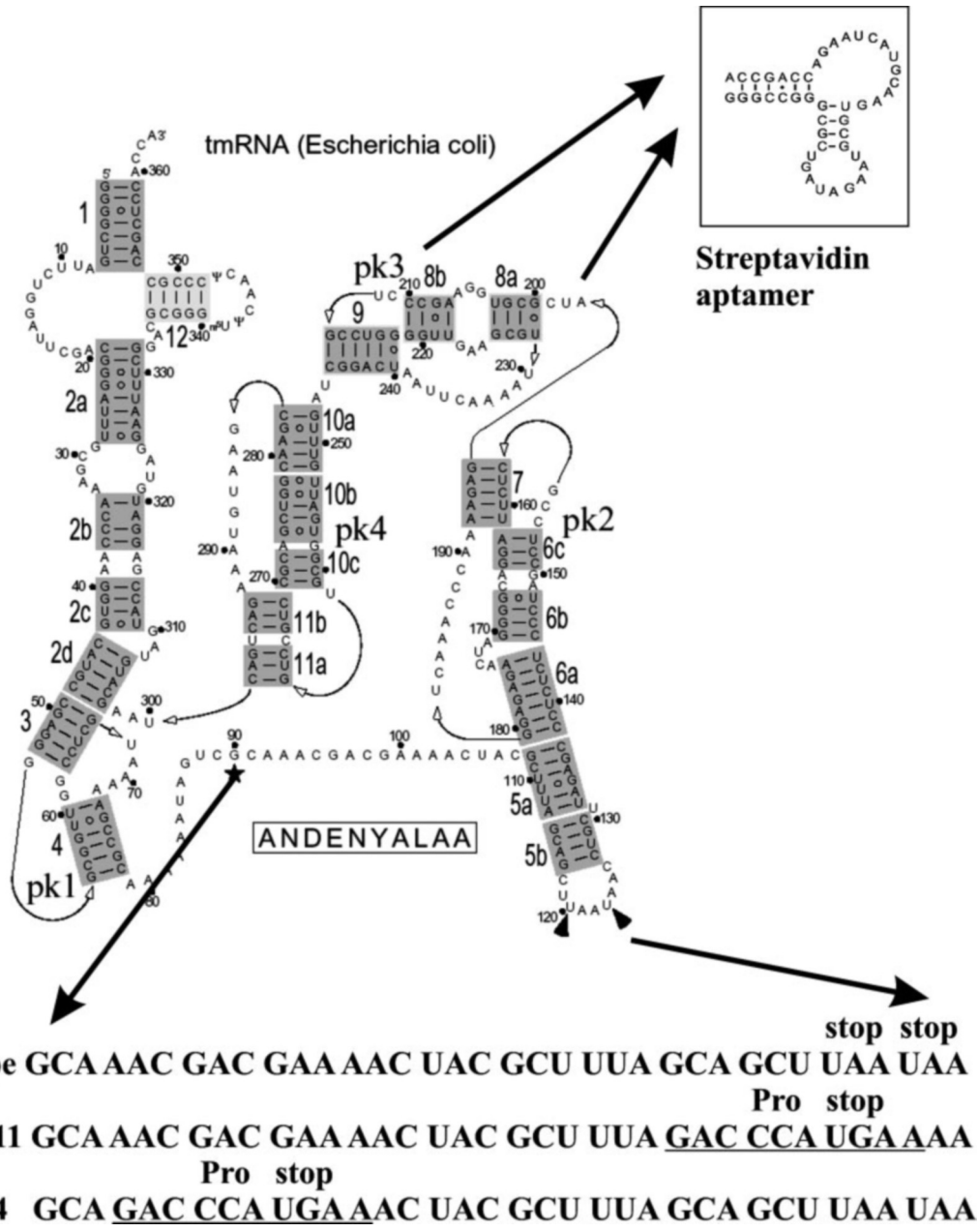


FIG. 1. **Secondary structure of tmRNA with numbered helices and pseudoknots (adapted from psyche.uthct.edu/dbs/tmRDB/tmRDB.html).** pk3 (nucleotides U212–A239) was substituted with an aptamer to streptavidin (*inset*). Mutations in the mRNA-like part of tmRNA are *underlined*.

specific positions during the termination of the *trans*-translation process. It is possible to block termination in the UGA stop codon recognized by RF2 if this release factor is inactive. The *E. coli* strain used in this study harbors a temperature-sensitive RF2 mutant that is active at 37 °C and significantly reduces activity at 42 °C (see "Experimental Procedures"). Wild-type tmRNA contains two UAA stop codons recognized by both release factors (RF1 and RF2). We mutated the first UAA stop codon to UGA in tmRNA-stra and changed the sequence around the stop codon (Fig. 1) to one known to be the "weakest termination signal" (31). To catch the complex at earlier stages of the passage of tmRNA through the ribosome we moved the UGA stop codon together with the weakest termination signal to the position of the fourth codon (pGEM-stra-4 expressing the mutant tmRNA-4) (Fig. 1, *tmRNA-4*). The presence of the UGA stop codon within the weakest termination context together with thermosensitive RF2 dramatically increased the probability of isolating the ribosome complexes containing mutant tmRNAs with the streptavidin tag affinity method.

*Confirming the System*—As designed, the system contains two altered elements: 1) mutant tmRNA with streptavidin aptamer instead of pk3 and a UGA stop codon recognized by RF2 and 2) a thermosensitive RF2 to impair termination at UGA. In the first series of experiments we tested the activity of mutant tmRNAs to determine whether they could tag proteins for subsequent proteolysis. To test the activity of tmRNA mutants we applied the Williams system (20), in which cells became resistant against kanamycin only in the presence of a functioning tmRNA upon IPTG induction of kanamycin resistance gene repressor. Fig. 2*A*, *left panel*, shows that all of the cells grew in the absence of IPTG and both mutants, tmRNA-4 and tmRNA-11, as well as without any tmRNA or the presence of wild-type tmRNA. However, only the cells lacking tmRNA were not viable in the presence of IPTG; the cells harboring wild-type or mutant tmRNA were alive (Fig. 2*A*, *right panel*). The results clearly show that the mutants tmRNA-4 and -11

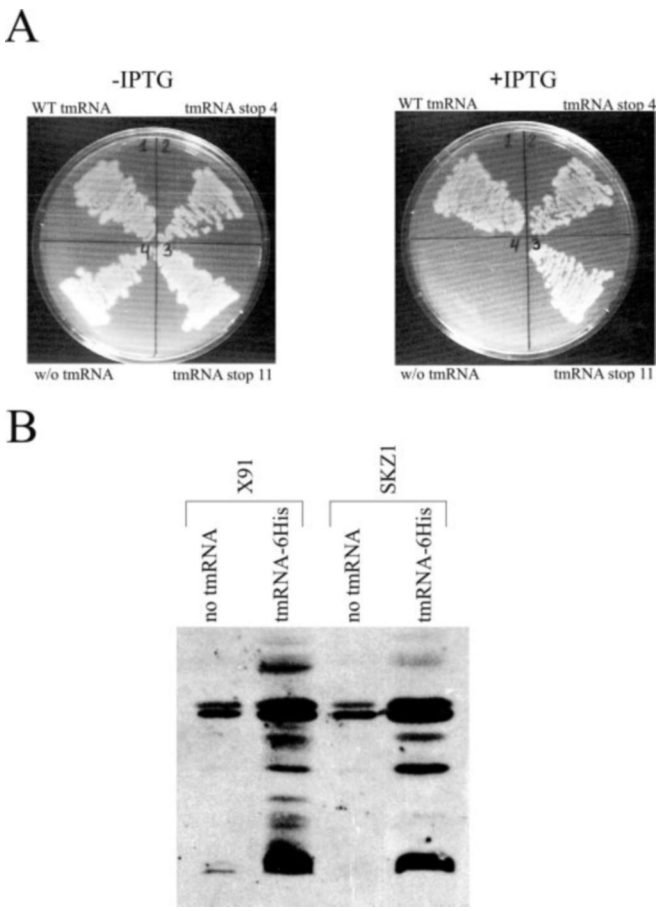


FIG. 2. **Mutant tmRNA in the presence of thermosensitive RF2 is functional *in vivo*.** *A*, the tagging activity of wild-type (*WT*) tmRNA and of mutant tmRNA-4 and -11 was tested in the Williams system (see "Experimental Procedures") using the strain X91 containing a wild-type RF2. Only cells containing a functional tmRNA can grow in the presence of IPTG (expression of truncated phage P22 Arc repressor mRNA). *B*, analysis of the tagged proteins using tmRNA-stra-($His_6$) within either the strain X91 with a wild-type RF2 or the strain SKZ1 with the thermosensitive RF2. Controls without (*w/o*) any tmRNA in the cells show the cross-reactivity of the ($His_6$)-antibody.

retain the tagging function that provides the degradation, although in the case of tmRNA-4 the degradation is lower because of the reduced sequence of the tag peptide (32).

In the second control experiment, we analyzed whether the SKZ1 strain producing temperature-sensitive RF2 supports the tmRNA tagging function. To this end we used a tmRNA with a streptavidin tag and an mRNA module that codes for $His_6$ residues instead of the last six amino acids. The latter feature reduces degradation of the tagged proteins (33) and thus allows identification of tagged proteins by commercially available anti-($His_6$) antibodies. This construct was introduced into cells lacking a functional tmRNA gene and containing either the wild-type RF2 (strain X91) or the thermosensitive RF2 (strain SKZ1). Fig. 2*B* demonstrates that the tagging pattern was very similar in both of the strains indicating normal activity of tmRNA in the SKZ1 strain. In the absence of any tmRNA, both strains showed the same background bands (34) that cross-reacted with the anti-($His_6$) antibody.

*The RNA Content of tmRNA·Ribosome Complexes*—RNA molecules were extracted from the isolated tmRNA·ribosome complexes and analyzed by gel electrophoresis as shown in Fig. 3*A*. The complex with tmRNA-4 blocked in the forth codon was obtained in good yield and found to contain tmRNA, 16 S, 23 S, and 5 S ribosomal RNAs (Fig. 3*A*, *lane 3*). Comparison of the 5 S rRNA, tmRNA, and tRNA bands densities from Fig. 3*A*, *lane 3*, indicated a molar ratio of ribosome to tmRNA of about 1:0.8 and that of tmRNA to tRNA of about 1:1. However, when tmRNA contained the affinity tag but a wild-type mRNA module (tmRNA-stra), almost no RNA could be observed (see the weak rRNA signals, Fig. 3*A*, *lane 6*). This indicates that the tmRNA-4-containing ribosomes are efficiently stalled with the stop codon in the A site and a $tRNA^{Pro}$ in the P site (see Fig. 1). Similarly, ribosomes containing wild-type tmRNA could not be isolated because of the efficient mRNA module translation and termination in the natural stop codon (compare Fig. 3*A*, *lanes 1* and *6*). Other controls including tmRNA-4 affinity isolated from the S30 (Fig. 3*A*, *lane 2*) and the initial fraction (after ribosome purification) and the flow-through (Fig. 3*A*, *lanes 4* and *5*, respectively) contain very small amounts of tmRNA, indicating the efficient enrichment of tmRNA·ribosome complex by the applied streptavidin tag method.

A potential tmRNA·ribosome complex stalled in the initiation stage unable to translate the mRNA module should be the same in the presence of both tmRNA-4 and tmRNA-stra. The fact that we do not observe a tmRNA band in *lane 6* (Fig. 3*A*) indicates that such a potential complex is negligible in the isolated tmRNA·ribosome complex. Scanning the tmRNA bands of Fig. 3*A*, *lanes 2*, *4*, and *3* (total tmRNA-4 in the S 30 cell-free extract, the tmRNA complexed with the ribosome in the initial ribosomal fraction, and tmRNA in the isolated complex, respectively) and considering the fraction volume applied to the gel revealed that at least 80% of tmRNA from the initial ribosomal fraction or 4% from total (S30 fraction) was bound to the ribosome in the isolated complex.

According to the nucleotide sequence of mutant tmRNAs (tmRNA-11 and tmRNA-4 in Fig. 1) the UGA stop codon should occupy the A site, and the CCA Pro codon should be in the P site. Therefore the tRNA bound to the P site of the ribosome should correspond to $tRNA^{Pro}$. To test this we probed the tRNA in the ribosome·tmRNA complex using Northern blot analysis with DIG-labeled DNA specific to $tRNA^{Pro}$. The results of the Northern blot for tRNA from the complexes blocked at either the 4th or the 11th codon are shown in Fig. 3*B*. The signal clearly demonstrates the presence of $tRNA^{Pro}$ in the complex. Rough estimation of the $tRNA^{Pro}$ amount was done by comparing the dot-blot signal intensities for $tRNA^{Pro}$ from the tmRNA-4 complex with known amounts of T7 $tRNA^{Pro}$ transcript (Fig. 3*C*). This approach did not allow us to make a quantitative estimation but indicated that most of tRNA in that complex was $tRNA^{Pro}$.

*Analysis of the Protein Content of tmRNA·Ribosome Complexes*—The proteins in the purified complexes containing tmRNA-4 and tmRNA-11 were separated by gel electrophoresis as shown in Fig. 4, *A*, *lane 3*, and *B*, *lane 3*, respectively). Ribosomal proteins of the 30 S (Fig. 4*A*, *lane TP30*) and 50 S subunits (Fig. 4*B*, *lane TP50*) served as markers. We used the following controls: (i) proteins from the initial ribosomal fractions of the complexes with tmRNA-4 and tmRNA-11 (*lanes 1* in Fig. 4, *A* and *B*, respectively) and (ii) proteins derived from flow-through fractions (*lanes 2* in Fig. 4, *A* and *B*). In the case of wild-type tmRNA no ribosomes were bound to the resin with the exception of at least three proteins from cell extract that were bound to the streptavidin resin. The corresponding bands are marked with *asterisks* at *lanes 3* in Fig. 4, *A–C*.

*Lanes 3* in Fig. 4, *A–C*, represent the analysis of protein content of the isolated complexes. The protein spectra in Fig. 4, *A* and *B*, show that complexes purified via tmRNA-4 and tmRNA-11 contain ribosomal proteins. The bands with the mobility corresponding to elongation factors G, Tu, and Ts (marked by *arrows* in *lane 1* of Fig. 4, *A* and *B*) disappear from the blocked complexes (*lane 3* in *both panels*). An additional

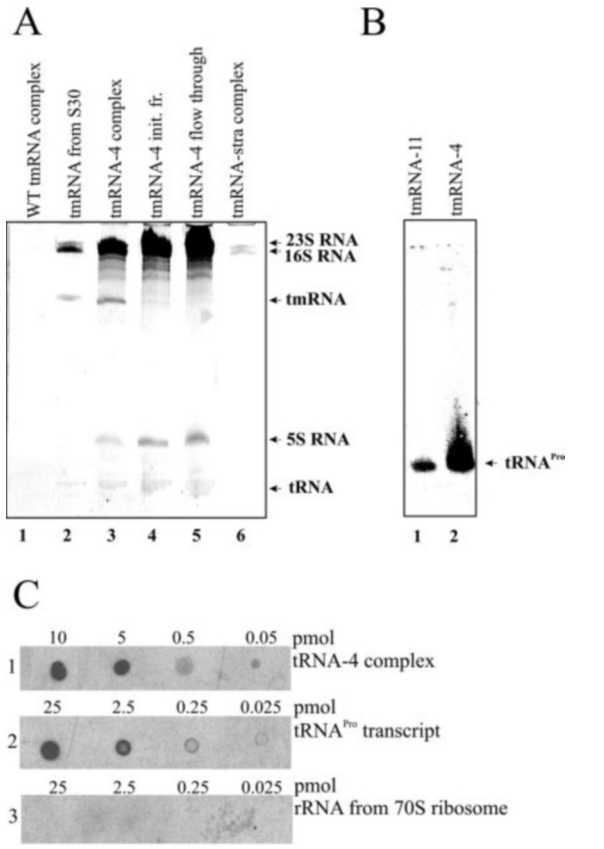


FIG. 3. **Analysis of the RNA content of the tmRNA·ribosome complexes.** *A*, electrophoretic separation of RNA isolated from the complex with wild-type (*WT*) tmRNA (*lane 1*) (1/20 of the total amount), tmRNA-4 isolated from S 30 cell-free extract by affinity chromatography (*lane 2*) (1/20 of the total amount), the complex with tmRNA-4 (*lane 3*) (1/20 of the total amount), the initial ribosomal fraction (*init. fr.*) (see "Experimental Procedures") (*lane 4*) (1/400 of the total amount), the flow-through fraction (the fraction of the ribosomes that did not bind to the column) (*lane 5*) (1/400), and the complex with tmRNA with the affinity tag and wild-type stop codon (tmRNA-stra) (*lane 6*) (1/20) in 5% denaturing PAGE. The positions of the RNAs are marked with the *arrows*. *B*, Northern blot probed with DIG-labeled DNA oligonucleotide complementary to $tRNA^{Pro}$ for RNA isolated from complexes carrying tmRNA-11 (*lane 1*) and tmRNA-4 (*lane 2*). *C*, dot blot of $tRNA^{Pro}$ from tmRNA-4 complex. *Blot 1*, tmRNA-4 complex (the loaded amounts in pmol are indicated). *Blot 2*, T7 transcript of $tRNA^{Pro}$ (amounts in pmol are indicated). *Blot 3*, total rRNA from the 70 S subunit in the same amounts.

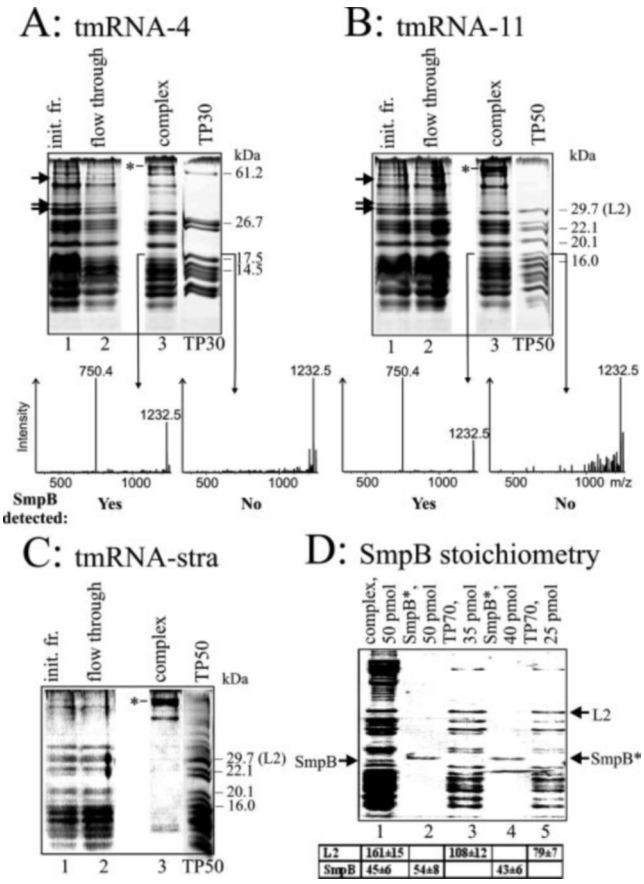


FIG. 4. **Analysis of the protein content of the tmRNA·ribosome complexes.** Electrophoretic separation of the proteins isolated from the complexes with tmRNA-4 (*A*) and tmRNA-11 (*B*) and tmRNA-stra (*C*) in 17.5% Tricine-SDS-PAGE. *Lane 1* (*init. fr.*), the initial ribosomal fraction (1/200 of the total amount). *Lane 2*, the flow-through fraction (1/200). *Lane 3* (*complex*), ribosomal fraction eluted from the streptavidin-Sepharose (tmRNA·ribosome complex) (1/10). *TP30* and *TP50*, the proteins isolated from small and large ribosomal subunits, respectively. In *A*, *B*, and *C*, the *asterisk* between *lanes 2* and *3* marks the position of a nonspecific band that was also detected in a control experiment with tmRNA lacking the affinity tag (not shown); in *A* and *B*, *arrows* indicate the position of putative translation factors; in *B* and *C*, on the *right*, the position of protein L2 is indicated. In *A* and *B*, the MALDI-ion trap MS/MS spectra below the gels were obtained from an hypothesis-driven multistage MS experiment testing for the presence of the characteristic peptide ion ANISDSYVLLR at *m/z* 1250.67 (detailed in Fig. 5) in the tryptic digest mixtures of the associated bands of A3, TP30, B3, and TP50 (*thin arrow lines*). The occurrence of the specific fragmentation signal at *m/z* 750.4 reveals the presence of SmpB. *D*, estimation of SmpB stoichiometry. *Lane 1*, complex with tmRNA-11, 50 pmol. *Lanes 2* and *4*, SmpB-$His_6$ (*SmpB**), 50 and 40 pmol, respectively. *Lanes 3* and *5*, TP70 (proteins isolated from 70 S ribosome), 35 pmol and 25 pmol, respectively. Positions of the proteins L2, SmpB, and SmpB-$His_6$ are marked by *arrows*. The *table* shows the scanned band intensities for L2 and SmpB in corresponding lanes.

protein band (18–19 kDa) appears in Fig. 4, *A* and *B*, *lane 3*, for the blocked complexes (best seen in *B*, used for MALDI analysis as described below) that could not be seen in the lanes for the other ribosomal fractions. The mobility of the new band corresponds to SmpB. In contrast, almost no ribosomal protein can be seen in the corresponding *lane 3* in Fig. 4*C*, indicating that no tmRNA·ribosome complex can be isolated from the cell in the case of tmRNA-stra with a wild-type termination signal.

The protein band with the mobility of SmpB (Fig. 4, *A* and *B*, *lanes 3*) was cut out and subjected to the enzymatic digestion and MALDI mass spectrometry. The results for the complex with tmRNA-11 are shown in Fig. 5. Peptide mass fingerprinting identified SmpB and ribosomal protein S7 as the main components of this band (Fig. 5). Our findings were confirmed by mass spectrometric fragmentation of selected peptides performed on a MALDI-ion trap using the same sample preparations. S7 was detected in the corresponding band from all four of the lanes analyzed, including in those of the ribosomal fractions TP50 and TP30 (data not shown).

The peptide mass fingerprinting data of the complex with the tmRNA-4 mutant was not sufficient to conclude whether or not SmpB was also present. Likewise, we could not detect SmpB in the same gel position of the control runs with TP30 and TP50 proteins. Thus, we established a characteristic peptide fragmentation signature for the tryptic SmpB peptide ANISDSYVLLR at *m/z* 1250.67. Resonant excitation of this peptide leads to an intense $y_6$ ion signal at *m/z* 750.4 caused by the preferred fragmentation of the peptide bond between aspartic acid and serine (*MS/MS inset* in Fig. 5). We collected and fragmented ions from all four of the samples in a hypothesis-driven multistage MS experiment (28) and noticed that the $y_6$ ion, indicative of the presence of SmpB, was obtained only from the complexes with the mutant tmRNA and not from the TP30 and 50 control samples (Fig. 4, *spectra* below *A* and *B*).

To estimate the molar ratio of ribosome:SmpB in the com-

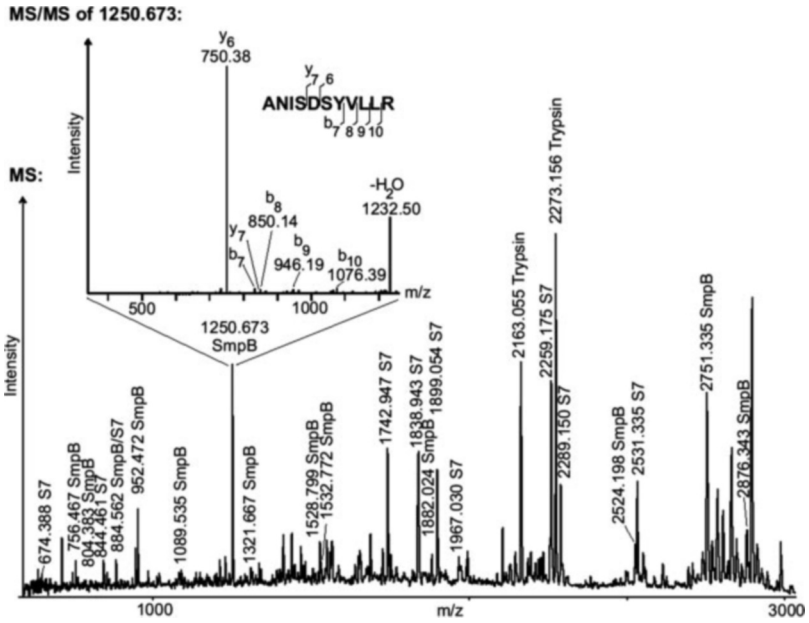


FIG. 5. **MALDI-quadrupole time-of-flight and MALDI-ion trap mass spectrometric analysis of the tryptic peptide mixture derived from a gel band that was suspected to contain SmpB (from the gel depicted in Fig. 4*B*, *lane 3*).** Monoisotopic masses and their assignment to peptides derived from the proteins S7, SmpB, and trypsin are shown. The *inset*, a MALDI-ion trap MS/MS spectrum, visualizes how the characteristic peptide fragmentation signature for the SmpB peptide ANISDSYVLLR was obtained. b and y ions, including the loss of water from the parent ions, are labeled. The most intense fragment ion signal was obtained from the $y_6$ ion at *m/z* 750.38 ± 0.30.

plex, certain amounts of purified SmpB-$His_6$ (SmpB*) protein and total proteins from the 70 S ribosome were applied to the Tricine-SDS-PAGE (Fig. 4*D*) and stained. Each band after the separation of 70 S ribosomal proteins in the gel (Fig. 4) contains more than one protein except for the bands of S1 and L2. L2 is a core ribosomal protein that is always present in the ribosome in equimolar amounts (35) We selected L2 as an internal standard for the ribosome:SmpB molar ratio estimation in the complexes. The intensities of the corresponding stained bands for SmpB and L2 were recorded (Table in Fig. 4*D*) both for control samples and tmRNA complexes. The stoichiometry of ribosome: SmpB was 1:0.8 in case of tmRNA-11 complex and 1:0.6 in case of tmRNA-4 complex. Because the tmRNA content of the latter complex was also about 0.8/70 S, we concluded that the ribosome complex contained near stoichiometric amounts of both tmRNA-4 and SmpB.

## DISCUSSION

Although the process of *trans*-translation has been studied for almost 10 years, the mechanism of the transition of tmRNA through the ribosome remains mainly unknown because previous studies with *in vitro* systems revealed only details of the initiation stage. In contrast, our study is based on *in vivo* systems that were successfully applied to gain mechanistic insights into the passage of tmRNA through the ribosome in *trans*-translation.

tmRNA is a highly structured molecule; in addition to numerous helices, *E. coli* tmRNA also has four pseudoknots (Fig. 1). Thus the question arises as to whether the ribosome unwinds these structural elements in the course of *trans*-translation or whether some of these structures are retained. It should be noted that pseudoknot structures are very stable and are not expected to be resolved easily by the ribosome. The pseudoknot presence in mRNA causes translational pausing, a process that can result in translation frameshifting (36). Recently we proposed that tmRNA can pass through the ribosome without destruction of its pseudoknots (19). We suggested that tmRNA should have a domain containing a structure imitating a codon-anticodon duplex that is recognized by the ribosomal A site. This domain should include the tRNA-like region of tmRNA and most probably pk1. The tRNA-like domain should move through the ribosome similar to a canonical tRNA using the same tRNA binding sites on the ribosome. At the same time the other pseudoknots should be located on the 30 S subunit outside of the decoding center. Helix 5, including the mRNA part of tmRNA, should be unwound during *trans*-translation. Accordingly, the structural rearrangements of tmRNA should take place, and tmRNA could easily leave the ribosome after the termination of *trans*-translation using the classical termination mechanism.

Recent structural studies of the SmpB complex using a tmRNA fragment that represented the tRNA-like domain showed structural similarity with the tRNA, although the angle between the arms is different in tmRNA (18). SmpB was shown to be necessary for the formation of a proper tmRNA structure recognized by the ribosomal A site. cryo-EM studies of the complex of tmRNA interacting with the ribosome in the pre-initiation stage in which the tRNA-like region of tmRNA remains in the complex with elongation factor Tu-GDP placed pk1 in the decoding center of ribosome. According to the cryo-EM model, another pseudoknot forms an arch-like structure in the 30 S subunit (17). This structure agrees well with our hypothesis. However, the arch-like structure in tmRNA that exists in the pre-initiation complex should undergo conformational changes during later stages of *trans*-translation. According to our model, after such rearrangement the pseudoknot 3 of tmRNA should be located on the solvent-accessible side of the ribosomal 30 S subunit. If we substitute pseudoknot 3 with another structural element, the aptamer to streptavidin, and if this element remains intact and is localized on the solvent-accessible surface of the 30 S subunit, it should allow binding the tmRNA·ribosome complex to streptavidin-Sepharose at different steps of *trans*-translation.

To test our hypothesis it was necessary to prepare such ribosome·tmRNA complexes in which *trans*-translation would be arrested at different steps of the passage of tmRNA through the ribosome. There are two strategies to obtain such complexes: 1) to use an *in vitro* system and 2) to stop *trans*-translation specifically within the cell and isolate the complex. *In vitro* systems were previously used to study the details of *trans*-translation only at the initiation stage (17). We decided to take advantage of the ability of the living cell to perform *trans*-translation very effectively and to isolate complexes of interest from the cell directly.

*trans*-Translation was stopped at the termination step in living cells. Together with the replacement of pk3 for the streptavidin aptamer, the coding region of tmRNA was mutated so that the termination signal could be recognized only by RF2. The codons

preceding the stop codon were changed to code for Asp and Pro, which were shown to decrease termination efficiency and provoke ribosome pausing (37). In our experiments these mutant tmRNAs were the only tmRNAs present in a strain that contained a thermosensitive RF2 inactivated at 42 °C. We varied the position of the mutant termination signal within the tmRNA sequence; to test early and later stages of *trans*-translation, the stop-codon UGA with its context described above was placed into the position of the 4th or 11th codon, respectively. Controls demonstrated that tmRNA-4 and tmRNA-11 were functional and that the isolated complexes did not contain significant amounts of initiation complexes. As a result we obtained two complexes in which tmRNA was tightly bound to the 70 S ribosome. The tmRNAs did not dissociate from the complex even after centrifugation through a sucrose gradient.

Such affinity purification is possible only when the proper structure of the RNA affinity domain is preserved and exposed outside the ribosome. Hence our successful isolation of tmRNA·ribosome complexes clearly indicates that the structure of the element that we have inserted into the position of pseudoknot 3 of tmRNA remains intact in both tmRNA-4 and tmRNA-11, which represent different stages of tmRNA passage through the ribosome. It follows that the ribosome does not unwind at least the structure of pk3 in the course of *trans*-translation, implying that this structural element is localized on the ribosome surface, on the solvent side of the 30 S subunit in agreement with cryo-EM data for the pre-initiation complex (17). These observations are in good agreement with our model for the path of tmRNA through the ribosome (19).

The analysis of the RNA content (Fig. 3) showed that rRNAs, $tRNA^{Pro}$, and tmRNA were components of the complex and presented in almost equimolar amounts indicating that when a stop codon was in the A site, a $tRNA^{Pro}$ was in the neighboring site (P site). Analysis of the protein content for the isolated complexes (Fig. 4) revealed that SmpB protein was in both tmRNA-4 and tmRNA-11 complexes.

Our results extend the knowledge about SmpB. This protein was found to be crucial for the *trans*-translation process (13, 14). It has been shown in a number of studies that SmpB can bind tmRNA, stimulating its aminoacylation (15). The structure of SmpB in the complex with a tmRNA fragment has been solved (18). According to cryo-EM data, SmpB is bound to tmRNA in the pre-accommodation complex (17). Recently, it was found that SmpB can also be bound to the ribosome (16) and that two molecules of SmpB pre-bound to one ribosome facilitate the accommodation of tmRNA in an *in vitro* system. These data indicate that SmpB plays an essential role at the stage of the initiation of *trans*-translation. We have shown that SmpB is also present in tmRNA·ribosome complexes at the different stages of tmRNA passage through the ribosome. Although we cannot exclude the rebinding of SmpB after dissociation from the initiation complex of tmRNA·ribosome, we can also consider the possibility that SmpB may remain bound to the tmRNA·ribosome complex after the initiation of the *trans*-translation process until termination. Our finding suggests that the action of SmpB may not be exclusively restricted to the initial stages of *trans*-translation but that it might also be important throughout the overall *trans*-translation process.

*Acknowledgments*—We are grateful to Dr. K. P. Williams for providing us with strain X91 and plasmid p6A and to Y. Teraoka for SmpB-$His_6$ protein. We also thank Prof. J. Dinman and S. V. Kiparisov for helpful discussions.

REFERENCES

1. Lee, S. Y., Bailey, S. C., and Apirion, D. (1978) *J. Bacteriol.* **133,** 1015–1023
2. Zwieb, C., Wower, I., and Wower, J. (1999) *Nucleic Acids Res.* **27,** 2063–2071
3. Keiler, K. C., Shapiro, L., and Williams, K. P. (2000) *Proc. Natl. Acad. Sci. U. S. A.* **97,** 7778–7783
4. Komine, Y., Kitabatake, M., Yokogawa, T., Nishikawa, K., and Inokuchi, H. (1994) *Proc. Natl. Acad. Sci. U. S. A.* **91,** 9223–9227
5. Ushida, C., Himeno, H., Watanabe, T., and Muto, A. (1994) *Nucleic Acids Res.* **22,** 3392–3396
6. Tu, G. F., Reid, G. E., Zhang, J. G., Moritz, R. L., and Simpson, R. J. (1995) *J. Biol. Chem.* **270,** 9322–9326
7. Gottesman, S., Roche, E., Zhou, Y. N., and Sauer, R. (1998) *Genes Dev.* **12,** 1338–1347
8. Keiler, K. C., Waller, P. R., and Sauer, R. T. (1996) *Science* **271,** 990–993
9. Rudinger-Thirion, J., Giege, R., and Felden, B. (1999) *RNA* (*N. Y.*) **5,** 1–4
10. Zvereva, M. I., Ivanov, P. V., Teraoka, Y., Topilina, N. I., Dontsova, O. A., Bogdanov, A. A., Kalkum, M., Nierhaus, K. H., and Shpanchenko, O. V. (2001) *J. Biol. Chem.* **276,** 47702–47708
11. Wower, I. K., Zwieb, C. W., Guven, S. A., and Wower, J. (2000) *EMBO J.* **19,** 6612–6621
12. Odom, O. W., Deng, H.-Y., Subramanian, A. R., and Hardesty, B. (1984) *Arch. Biochem. Biophys.* **230,** 178–193
13. Karzai, A. W., Susskind, M. M., and Sauer, R. T. (1999) *EMBO J.* **18,** 3793–3799
14. Hanawa-Suetsugu, K., Takagi, M., Inokuchi, H., Himeno, H., and Muto, A. (2002) *Nucleic Acids Res.* **30,** 1620–1629
15. Barends, S., Karzai, A. W., Sauer, R. T., Wower, J., and Kraal, B. (2001) *J. Mol. Biol.* **314,** 9–21
16. Hallier, M., Ivanova, N., Rametti, A., Pavlov, M., Ehrenberg, M., and Felden, B. (2004) *J. Biol. Chem.* **279,** 25978–25985
17. Valle, M., Gillet, R., Kaur, S., Henne, A., Ramakrishnan, V., and Frank, J. (2003) *Science* **300,** 127–130
18. Gutmann, S., Haebel, P. W., Metzinger, L., Sutter, M., Felden, B., and Ban, N. (2003) *Nature* **424,** 699–703
19. Ivanov, P. V., Zvereva, M. I., Shpanchenko, O. V., Dontsova, O. A., Bogdanov, A. A., Aglyamova, G. V., Lim, V. I., Teraoka, Y., and Nierhaus, K. H. (2002) *FEBS Lett.* **514,** 55–59
20. Williams, K. P., Martindale, K. A., and Bartel, D. P. (1999) *EMBO J.* **18,** 5423–5433
21. Bjornsson, A., and Isaksson, L. A. (1996) *Nucleic Acids Res.* **24,** 1753–1757
22. Platt, T., Mueller-Hill, B., and Miller, J. H. (1972) in *Experiments in Molecular Genetics* (Miller, J. H., ed) pp. 352–355, Cold Spring Harbor Laboratory, Cold Spring Harbor, NY
23. Srisawat, C., and Engelke, D. R. (2001) *RNA* (*N. Y.*) **7,** 632–641
24. Rheinberger, H.-J., Geigenmuller, U., Wedde, M., and Nierhaus, K. H. (1988) *Methods Enzymol.* **164,** 658–672
25. Nowotny, P., Nowotny, V., Voss, H., and Nierhaus, K. H. (1988) *Methods Enzymol.* **164,** 131–147
26. Schagger, H., and von Jagow, G. (1987) *Anal. Biochem.* **166,** 368–379
27. Krutchinsky, A. N., Kalkum, M., and Chait, B. T. (2001) *Anal. Chem.* **73,** 5066–5077
28. Kalkum, M., Lyon, G. J., Chait, B. T. (2003) *Proc. Natl. Acad. Sci. U. S. A.* **100,** 2795–2800
29. Leonov, A. A., Sergiev, P. V., Bogdanov, A. A., Brimacombe, R., and Dontsova, O. A. (2003) *J. Biol. Chem.* **278,** 25664–25670
30. Nameki, N., Tadaki, T., Himeno, H., and Muto, A. (2000) *FEBS Lett.* **470,** 345–349
31. Bjornsson, A., Mottagui-Tabar, S., and Isaksson, L. (1996) *EMBO J.* **15,** 1696–1704
32. Flynn, J. M., Levchenko, I., Seidel, M., Wickner, S. H., Sauer, R. T., and Baker, T. A. (2001) *Proc. Natl. Acad. Sci. U. S. A.* **98,** 10584–10589
33. Roche, E. D., and Sauer, R. T. (2001) *J. Biol. Chem.* **276,** 28509–28515
34. Mukherjee, S., Shukla, A., and Guptasarma, P. (2003) *Biotechnol. Appl. Biochem.* **2,** 183–186
35. Rohl, R., and Nierhaus, K. H. (1982) *Proc. Natl. Acad. Sci. U. S. A.* **79,** 729–733
36. Tu, C., Tzeng, T. H., and Bruenn, J. A. (1992) *Proc. Natl. Acad. Sci. U. S. A.* **89,** 8636–8640
37. Hayes, C. S., Bose, B., and Sauer, R. T. (2002) *J. Biol. Chem.* **277,** 33825–33832